New shear apparatus for in situ small-angle x-ray scattering experiments

Ch. Münch and J. Kalus

Citation: Review of Scientific Instruments **70**, 187 (1999); doi: 10.1063/1.1149564
View online: http://dx.doi.org/10.1063/1.1149564
View Table of Contents: http://scitation.aip.org/content/aip/journal/rsi/70/1?ver=pdfcov
Published by the AIP Publishing

New shear apparatus for *in situ* small-angle x-ray scattering experiments

Ch. Münch and J. Kalus[a)]
Experimentalphysik I, Universität Bayreuth, D-95440 Bayreuth, Germany

(Received 9 December 1996; accepted for publication 23 October 1998)

Small-angle scattering is a powerful tool for the investigation of micellar solutions. By applying a shear flow, increased information can be obtained. A new parallel disks shear apparatus for *in situ* detection of the sheared state by means of small-angle x-ray scattering is described. The steady shear rate Γ may be changed from 0.25 to 200 s^{-1}. If needed transient shear rates Γ having the shape of stop and go, being sinusoidal or a ramp, can be applied. Typical response times of the apparatus are less than 1 s. The path length of the x rays in the shear cell can be continuously changed between 0.5 and 5 mm. The angle α between the incident x-ray beam and the shear gradient vector $\mathbf{\Gamma}$ may be varied from 0° to approximately 55°. As an example, we give a brief report of experiments performed on two sheared aqueous surfactant solutions with differently shaped (disk-like and rod-like) particles: a 30% by weight solution of tetramethylammonium perfluorononanoate in D_2O and a 30 mM solution of tetraethylammonium perfluorooctanesulfonate in H_2O. © *1999 American Institute of Physics.* [S0034-6748(99)04501-3]

I. INTRODUCTION

In the past, many small-angle scattering experiments with light (SALS), neutrons (SANS), and x rays (SAXS) have been used to examine liquid crystals as well as viruses, polymers, and micelles in solution. For such investigations, neutrons are widely used but most of the information can also be obtained by x rays. Although under normal conditions they are not suitable for contrast variation experiments, they have one great advantage compared to neutrons: One does not depend on a neutron source! X-ray machines (with powers up to 10 kW) can be found in many laboratories. Therefore we decided to develop a new shear apparatus for SAXS experiments, despite the fact that several shear cells are described in the literature.

The most common geometries used to create shear flows are shown in Fig. 1:[1] sliding plates[2–4] [Fig. 1(a)], concentric cylinders [Couette flow,[5–18] Fig. 1(b)], cone and plate[19,20] [Fig. 1(c)], and parallel disks[21–30] [Fig. 1(d)]. All four types have been used in small-angle scattering experiments.

In most cases the incident beam with wave vector $\mathbf{k}$ ($|\mathbf{k}|=2\pi/\lambda$, λ is the wave length of the incident beam) is parallel or perpendicular to the shear gradient $\mathbf{\Gamma}$ and perpendicular to the velocity vector $\mathbf{v}$. However, for some detailed investigations of the scattering intensity distribution the angle α between $\mathbf{\Gamma}$ and $\mathbf{k}$ should differ from 0° or 90°. Since too large path lengths d of the beam in the sample lead to multiscattering, which may cause problems, d is typically of the order of millimeters.

II. SHEAR APPARATUS

The demand for continuous motion makes it impossible to use a sliding plates shear cell. (Sampling times for neutron or x-ray small-angle scattering experiments may extend to several days.) For investigations where $\mathbf{k}$ is parallel to $\mathbf{\Gamma}$ and perpendicular to $\mathbf{v}$, the Couette, the cone and plate, and the parallel disks geometry are favorable. In the Couette cell the incident beam passes through the sample twice, but both $\mathbf{v}$ and $\mathbf{\Gamma}$ reverse direction, which may be inconvenient if $\mathbf{k}$ by some reasons is chosen not to be parallel to $\mathbf{\Gamma}$.

The geometry of cone and plate and the parallel disks differ in the spatial dependence of the shear gradient. The magnitude of the shear gradient is defined as $\Gamma=v/d$. v is the velocity of the moving plate and d the distance between the plates, respectively. In the parallel disk geometry, v depends on the distance r to the axis of rotation and on angular velocity ω: $v=\omega r$. Therefore Γ varies with ω and r. In contrast, in the cone and plate geometry, both v and d change linearly with r, leading to a shear gradient depending only on ω.

We decided to construct a shear cell according to Fig. 1(d). Two parallel plates (henceforth called windows), one fixed and the other rotating with an angular velocity $\boldsymbol{\omega}$, result in a velocity field $\mathbf{v}=\boldsymbol{\omega}\times\mathbf{r}$ depending on the distance $\mathbf{r}$ from the axis of rotation. In many cases, $\mathbf{k}$ may be chosen parallel or antiparallel to $\mathbf{\Gamma}$, respectively.

For the construction of the SAXS shear apparatus, various conditions had to be fulfilled:

(a) The apparatus must function for measurements in which the angle α between the axis of rotation (i.e., the direction of the shear gradient $\mathbf{\Gamma}$) and the incident x-ray beam can be changed between $0\leqslant\alpha\leqslant55°$;
(b) In order to facilitate measurements with $\alpha\neq0°$, no absorbing parts such as a driving axle should disturb the incoming as well as the scattered beams;
(c) The x-ray absorption and scattering power of the windows must be minimalized. Hence the thickness of the windows should be as small as possible and they should be made of a material with low atomic number since the coefficient of x-ray absorption is small for elements with low atomic number;

a)Electronic mail: kalus@btp1×1.phy.uni-bayreuth.de

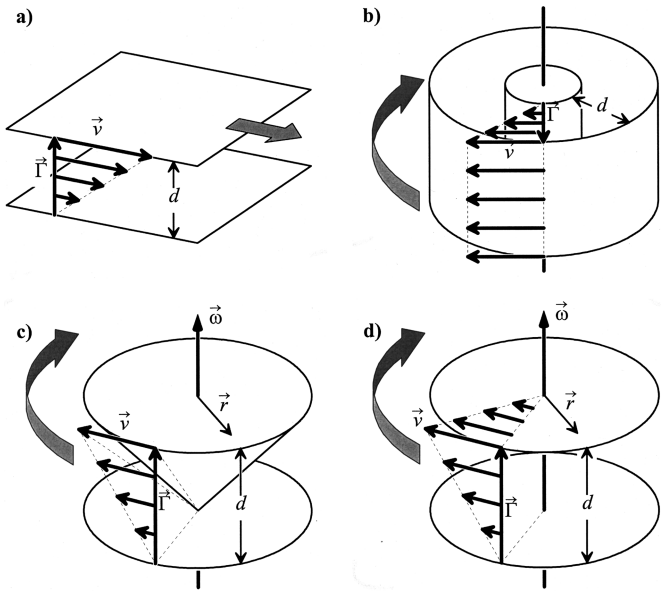

FIG. 1. Common shear flow geometries: (a) sliding plates; (b) concentric cylinders (Couette flow); (c) cone and plate; (d) parallel disks (Ref. 1).

(d) Since the diameter of the pinhole collimated x-ray beam of a SAXS apparatus is typically around 1 mm, the distance between the beam and the axis of rotation should be $r \geqslant 10$ mm to get a nearly linear velocity field over the cross section of the x-ray beam. Then the curvature of the velocity vector **v** as well as the dependence of Γ on r can both be neglected;
(e) Big sealings of moving parts are much easier to handle if they seal in a radial direction instead of an axial direction. Therefore we chose a radial shaft packing as the main sealing;
(f) Friction bearings are used as they normally cause less vibration than ball bearings or roller bearings;
(g) The movement of a stepping motor is transmitted by a toothed belt to the shear apparatus. This belt reduces the vibration related to the motor's steps;
(h) An electronic stepping motor control unit was used allowing, for example, steady, stepwise or sinusoidal motions of the stepping motor;
(i) The thickness of the sample should be adjustable without dismantling the shear apparatus. This facilitates finding an optimal thickness for different samples and different x-ray energies;
(j) The material of the apparatus should be resistant to as many chemicals as possible. Therefore we have chosen Viton sealings and high-grade steel for all metallic parts (except the windows) which are in contact with the sample; and
(k) To allow measurements at different temperatures, the shear apparatus is equipped with heating and cooling devices.

A cross section of the SAXS shear apparatus (in scale) is shown in Fig. 2. The steel rotator (3) moves between two aluminum frames (1), both fixed to a base plate (2). The two friction bearings (4) for the steel rotator are self-oiling, each consisting of a stainless steel bushing (5) shrunk into one of the fixed aluminum frames (1), and a brass bushing (6) shrunk onto the steel rotator (3). They are lubricated by resin-free oil, fed through a borehole on the top of the aluminum frames (1) (not shown). The oil is distributed by means of two circular grooves (also not shown). The liquid sample is enclosed between two parallel, x-ray-transparent plates, the so-called x-ray windows (7 and 8). (Details of the construction of the windows are given in Fig. 3.) The revolving window (7) is screwed to the steel rotator (3) and is sealed by a Viton ''O'' ring (9). The fixed window (8) is screwed to the steel frame ring (10), again sealed by a Viton O ring (9). The steel frame ring (10), in turn, is screwed on to a linear stage (11) bolted to the base plate (2). The stage (11) can be positioned by a micrometer gauge (12), allowing movement of the steel frame ring (10) and the fixed window parallel to the axis of rotation. By this movement, the width of the gap d between the two x-ray windows (7) and (8) can be varied between 0.5 and 5 mm, affording the possibility of performing experiments under each sample's optimum conditions. In addition, the fixed steel frame ring (10) is screwed to a steel ring (13) which supports a commercial Viton radial shaft packing (14) (*Busak and Luyken* AD $70\times90\times10$ mm). Its sealing edge fits to the hardened surface of the steel rotator inlay (15) without any need of lubrication. [The steel rotator inlay (15) is screwed to the steel rotator (3).] The radial shaft packing (14) seals sample liquids in the shear cell without significant leakage. A toothed ring (16) which finally transmits the torque from the stepping motor via a toothed belt is screwed to the steel rotator (3).

Two boreholes through the steel frame ring (10) serve as air (17) and filling duct (18) of the shear cell, respectively. Each is closed with a Teflon-coated rubber foam plug. The shear cell is filled with liquids by means of a syringe with a needle penetrating the self-sealing foam plug.

The temperature of the apparatus and the sample is controlled by an external thermostat circulating water through boreholes in the two aluminum frames (1) (these boreholes are not shown). Two platinum resistors PT100 are fixed to these frames. One of these resistors is used to regulate the temperature at this point within an accuracy of ±0.1 °C. The temperature of the sample liquid itself is also measured by a third PT100, introduced through the air duct (17). Furthermore, electric heating foils (*Minco* HK 5166 R 529 L12 A, 220 V, 529 Ω) can be attached to the aluminum frames (1) to readily allow measurements at elevated temperatures. The device operates safely between 0 and 60 °C, to an absolute accuracy of better than 0.5 °C, as measured by the Pt 100 introduced through the air duct. This accuracy and the absolute value of the temperature measured in the liquid, which is continuously monitored, depends on the difference between the temperature of the sample and ambient temperature, as well as on the heat release in the liquid caused by friction. The latter depends on shear Γ and on viscosity. Temperatures above 60 °C cannot be reached because thermal expansion increases the friction of the bearings.

The construction of the two x-ray windows turned out to

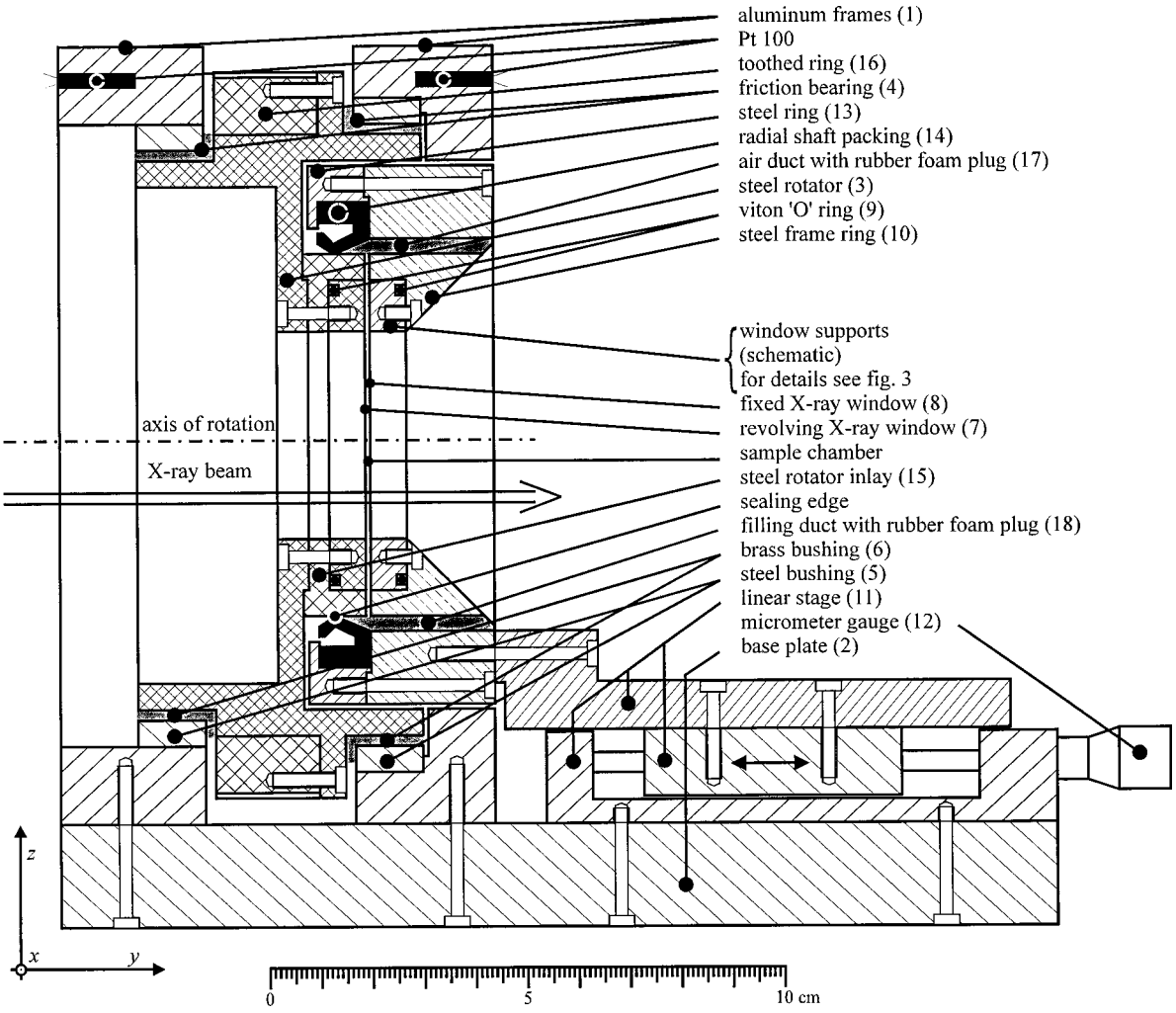

FIG. 2. Cross section of the x-ray shear apparatus (in scale). The apparatus (with exception of the base plate, the linear stage, the aluminium frames, and the air and filling duct) is radially symmetric to the axis of rotation. The *x*, *y*, and *z* axes build up a system of coordinates, coinciding with that in Fig. 5. Rotating parts are drawn in checked pattern.

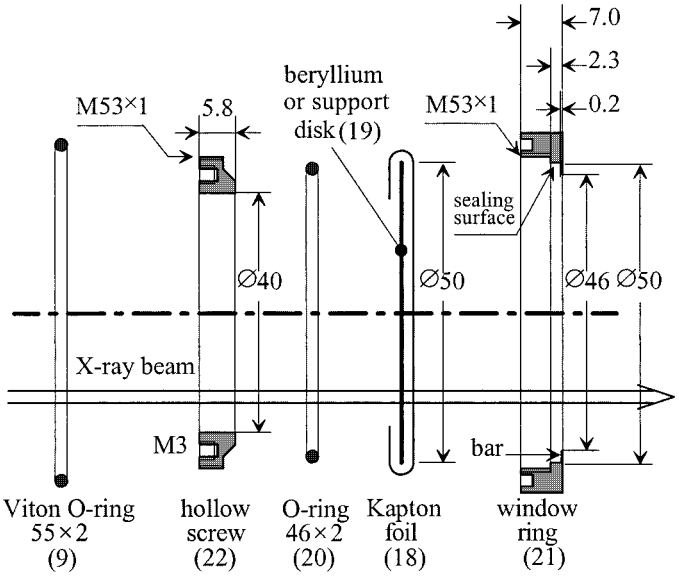

FIG. 3. Exploded view of the steel window ring and the beryllium plate or brass support disk covered by the Kapton foil (in scale). All measurements in millimeters.

be a serious problem. Because of its low x-ray absorption, we used beryllium as window material. But, due to chemical corrosion, direct contact of beryllium and surfactant solutions must be avoided. (It is known that even water leads to corrosion on beryllium.[31])

While elsewhere a 5 μm polyimide film coating was used to protect the beryllium,[32] we used a 12.5 μm Kapton foil. As indicated in Fig. 3, this foil (18) was laid tight over a 0.1 mm beryllium disk (19) and folded over the beryllium edge to the back side. The O ring 46×2 (20) seals in the axial direction against the covered beryllium disk, as well as in the radial direction against the inner wall of the steel window ring (21). By means of the hollow steel screw (22), the O ring (20) is pressed with brute force to the Kapton foil (18), beryllium disk (19), and window ring (21). Amazingly the soft O ring (20) sealed this window perfectly despite the existence of wrinkles in the Kapton foil. This construction works well without leakage, but does not allow *in situ* optical control of the sample.

In a second version, we replaced the beryllium disk by a support disk made of 0.5 mm brass with windows milled in it. Its shape is shown in Fig. 4. Provided that the Kapton foil

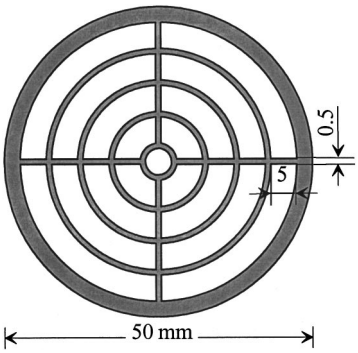

FIG. 4. Front view (in scale) of the brass disk which supports the Kapton foil x-ray windows. The thickness of the disk is 0.5 mm. All measurements in millimeters.

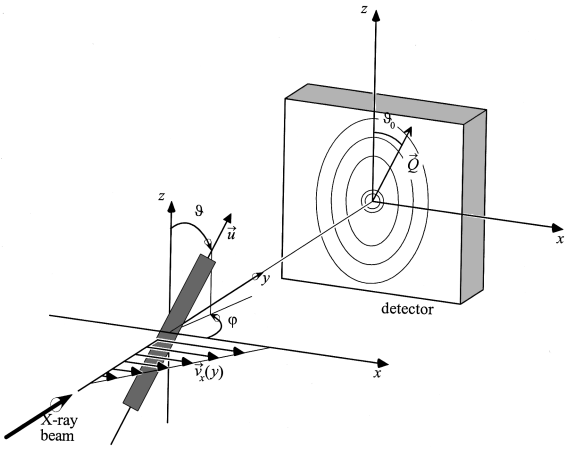

FIG. 5. Experimental setup of the small-angle, x-ray camera with the shear apparatus. *x*, *y*, and *z* and ϑ and φ are Cartesian and spherical systems of coordinates, respectively. $\mathbf{v}_x(y)$ is the velocity field (which may point in the *z* direction as well), as generated by the shear apparatus. Furthermore, the unit orientation vector $\mathbf{u}$ of a rod-like particle and the scattering vector $\mathbf{Q}$, lying approximately in the $x-z$ plane, is indicated. The shear gradient $\boldsymbol{\Gamma}$ and the x-ray beam are oriented in the *y* direction.

was mounted correctly, the smoothness of the flat foil was better than 0.1 mm. By this method, the x-ray absorption of the beryllium can be avoided (the absorption of the Kapton is $\approx$1%), and an optical inspection of the liquid sample is possible. If the rotator revolves, the cross bars of the support disk occasionally pass through the x-ray beam. But under most experimental conditions, this does not affect the measurements.

When performing shear experiments, one must know the exact value of the shear gradient Γ. It depends on the angular velocity ω of the revolving plate, the distance r of the x-ray beam from the axis of rotation, and the sample thickness d:

$$\Gamma = \frac{v}{d} = \frac{\omega r}{d}. \tag{1}$$

ω is calculated from the motor stepping rate which can be measured very exactly. The base plate (2) of the shear apparatus is mounted on a support (not shown in Fig. 1) which can be shifted by means of another linear stage. Thus, r can be determined to an accuracy of ± 0.025 mm. A problem is the calibration of d, because it cannot be measured directly. Nevertheless, its accurate determination is important. An inaccuracy of 0.1 mm, for example, typically gives an error of 10% in Γ (as d is usually 1 mm). This problem has been solved by a calibration via the sample volume V enclosed in the shear apparatus. V has been determined by filling the sample cell with water by means of a calibrated syringe and using d spacers of 1.0, 1.45, 3.0, and 4.0 mm between the x-ray windows (7) and (8) for calibration. Thus, a calibration of V against d and against the scale of the micrometer gauge (12) can be performed, giving a relative accuracy of about 2% for $d \geqslant 1$ mm.

As mentioned before, the shear apparatus is driven by a stepping motor (*Bautz* HY 200-3437-460A8, microstepping modus: 2000 steps per revolution, maximum torque: 2.25 nm at $\approx$1500 steps/s). If r, the distance between the axis of rotation and the x-ray beam amounts to $r = 10$ mm and the sample thickness is $d = 1$ mm, a shear gradient of $\Gamma_{\max} \approx 200\ \mathrm{s}^{-1}$ can be obtained. Since very low Γ values are connected with low motor stepping rates, a continuous motion of the rotator is possible only above $\Gamma_{\min} \approx 0.25\ \mathrm{s}^{-1}$ where the stepping rate is typically around 25 Hz. Of course, this limit can be different for different stepping motors. Due to the reduced torque of the stepping motor at start, the maximum shear rate of start-stop experiments is limited to $\Gamma_{\max} \approx 80\ \mathrm{s}^{-1}$.

The mutual arrangement of the shear apparatus and the two-dimensional electronic detector for the special case where the x-ray beam is parallel to $\boldsymbol{\Gamma}$ can be seen in Fig. 5. $\boldsymbol{\nu}_x(y)$ is the velocity field created by the shear apparatus at the point where the x-ray beam penetrates the sample. Figure 5 shows the case where the beam hits the window vertically above or below the axis of rotation. The spherical coordinates ϑ and φ are useful to describe the orientation of particles (having an axis of revolution defined by the unit vector $\mathbf{u}$). The isointensity lines on the detector symbolize a typical scattering pattern (compare Fig. 7). The scattering vector $\mathbf{Q}$, which lies approximately in the detector plane, is the momentum transfer of the scattered radiation. Its modulus is given by $(4\pi/\lambda)\sin(\Theta/2)$, where Θ is the scattering angle.

The system of coordinates shown in Fig. 5 is the same as indicated in Figs. 2, 6, and 7. It can also be used for the theoretical evaluation of the orientation of the rod-like particles by means of an orientational distribution function, described in Sec. III.

III. MEASUREMENTS

The theoretical description of small-angle scattering is well known. The scattered intensity $I(\mathbf{Q})$ of monodispersed particles can be calculated as follows:[33]

$$I(\mathbf{Q}) = C[F^2(\mathbf{Q})]S(\mathbf{Q}). \tag{2}$$

C is a proportionality factor, $S(\mathbf{Q})$ is the structure factor, which is related to the correlation between the particles, and $F(\mathbf{Q})$ is the form factor, representing the scattering due to a single particle. The angular brackets indicate a mean value with respect to all orientations of the particles. For particles having an axis of revolution we get

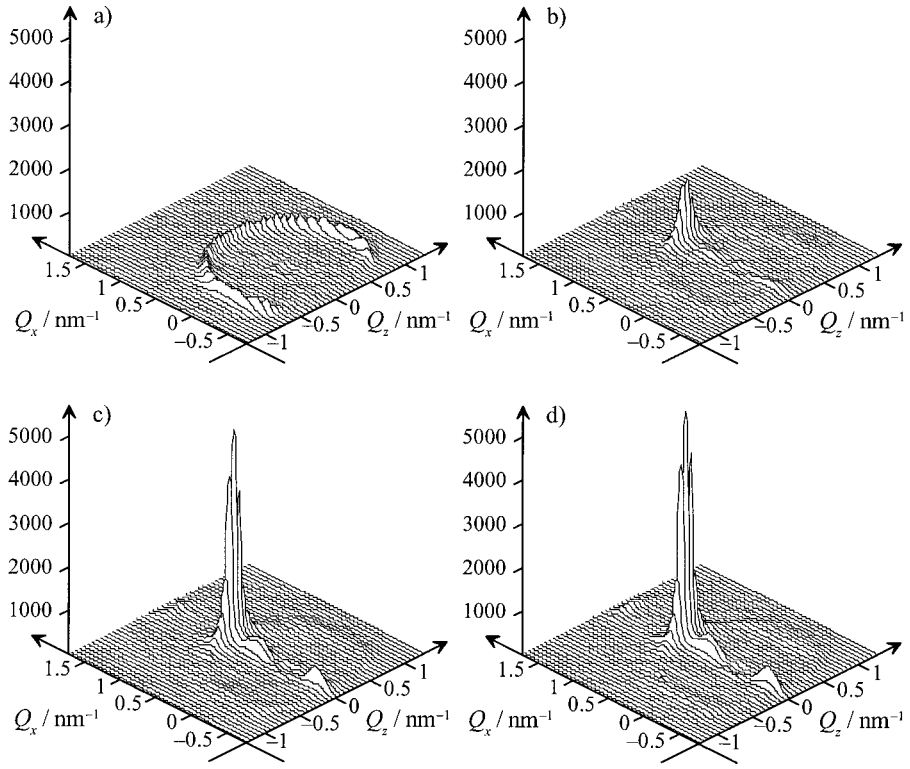

FIG. 6. Scattered intensity distribution of a sheared, 30%-by-weight solution of TMPFN in D_2O at a temperature of 34 °C. A shear rate of $\Gamma = 6\ s^{-1}$ (with flow velocity v in Q_z direction) starts at $t = 0$; the sampling times are 200 s. (a) The unsheared solution in the interval [−200 s, 0]; (b) [0, 200 s]; (c) [200 s, 400 s], and (d) [400 s, 600 s]. The depression in intensity around $Q_x = Q_z = 0$ is due to the beamstop.

$$[F^2(\mathbf{Q})] = \int_0^{2\pi} \int_0^{\pi} f(\vartheta, \varphi) |F(\mathbf{Q}, \vartheta')|^2 \sin \vartheta \, d\vartheta \, d\varphi, \tag{3}$$

where ϑ' is the angle between the scattering vector $\mathbf{Q}$ and the direction of the axis of revolution of the particle $\mathbf{u}$; ϑ' is a function of ϑ and φ (see Fig. 5). f is the orientational distribution function and may depend on $\mathbf{\Gamma}$ and time and influences the measured scattering intensity distribution. We present two examples for isotropic as well as anisotropic scattering patterns. All experiments have been carried out with the shear apparatus described above using a small-angle x-ray scattering apparatus, the features of which are given in Ref. 34.

The first example is a 30% by weight solution of tetramethylammonium perfluorononanoate (TMPFN; $N(CH_3)_4{}^+ - C_8F_{17}COO^-$) in D_2O. At a temperature of 34 °C, this sample exhibits a discotic nematic phase.[35] Figure 6 shows the development of the scattering pattern (and thus the orientational state) after switching on a shear gradient of $\Gamma = 6\ s^{-1}$ (with flow velocity v in z direction, see Fig. 5) at $t = 0$. The three-dimensional intensity plots show the scattered intensity $I(Q)$ accumulated within 200 s by a position-sensitive detector, i.e., as a function of the scattering vector $\mathbf{Q}$. Notice that the scattering patterns of Fig. 6 are radially symmetric with respect to $Q_x = Q_z = 0$.

One can see how the isotropic scattering pattern in the undisturbed state [Fig. 6(a)] becomes increasingly anisotropic with time. This evidently indicates the increasingly oriented state of the disk-shaped particles.

The second example is a 30 mM solution of tetraethylammonium perfluorooctanesulfonate (TEPOS; $N(C_2H_5)_4{}^+ - C_8F_{17}SO_3{}^-$) in H_2O. At a temperature of 25 °C rod-like particles with a radius of $R = 2.14$ nm exist in the solution.[36] In Fig. 7, scattering intensity distribution of the unsheared sample [Fig. 7(a)] can be compared to that of the sheared one [Fig. 7(b)] at $\Gamma = 180\ s^{-1}$. The contour plots show the scattered intensity $I(\mathbf{Q})$ as measured by the position-sensitive detector. Sampling times are 20 h in the unsheared state and 1 h at $\Gamma = 180\ s^{-1}$, respectively. The origin of the system of coordinates $Q_x = Q_z = 0$, is now located in the center of the detector and is covered by a beam stop. The deformation of the contour lines belonging to the sheared solution is evident. This indicates the existence of an alignment of the axis of the rod-like micelles along the Q_x direction.

We observed an extra scattering intensity when the x-ray beam hits the edge of the radial bar of the support disk (see Fig. 4). This intensity is concentrated below $Q \approx 0.1\ nm^{-1}$ and can, if disturbing, easily avoided by a proper gating of the electronic counter. It is not the aim of this report to give a detailed evaluation of the presented measurements. This

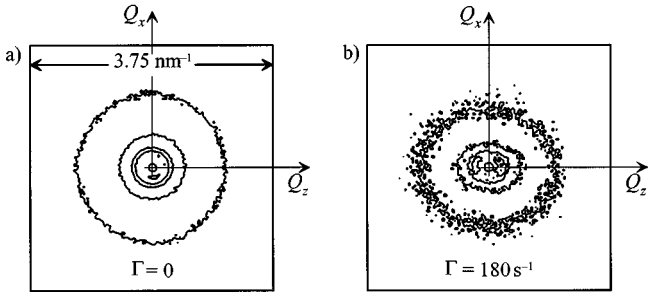

FIG. 7. Contour plots of the scattered intensity distribution of a 30 mM solution of TEPOS in H_2O at a temperature of 25 °C. (a) A measurement at $\Gamma = 0$ (recording time: 20 h). The intensities of the contour lines are (from the outside to the inside) 400, 1400, 2400 3400, 4400, and 400. (b) A measurement at $\Gamma = 180\ s^{-1}$ (flow velocity v in Q_x direction, recording time: 1 h). The intensities of the contour lines are 20, 70, 120, 170, and 20. The depression around $Q_x = Q_z = 0$ is due to the beamstop.

will be given in a forthcoming article. But we would like to point out, that it is possible to reproduce the measured scattering patterns using distribution functions $f(\vartheta,\varphi)$ as obtained by theoretical considerations.

We have demonstrated that the x-ray shear apparatus works reliably and that it is possible to detect the sheared state *in situ* by means of small-angle x-ray scattering. We mention again that experiments where the x-ray beam penetrates the sheared sample at angles $0<\alpha<55°$ with respect to the axes of rotation (as discussed in Ref. 24) are also possible with this setup.

ACKNOWLEDGMENTS

The support of the machine shop of the University of Bayreuth, where the shear apparatus was built, as well as the aid of W. Griess, concerning software and hardware problems, is gratefully acknowledged.

[1] C. W. Macosko, *Rheology: Principles, Measurements, and Applications* (VCH, New York, 1994), p. 183.
[2] K. A. Koppi, M. Tirrell, F. S. Bates, K. Almdal, and R. H. Colby, J. Phys. II **2**, 1941 (1992).
[3] Y. Zhang and U. Wiesner, J. Chem. Phys. **103**, 4784 (1995).
[4] S. Okamoto, K. Saijo, and T. Hashimoto, Macromolecules **27**, 5547 (1994).
[5] M. M. Couette, Ann. Chem. Phys. Ser. VI **21**, 433 (1890).
[6] K. H. de Haas, D. van den Ende, C. Blom, E. G. Altena, G. J. Beukema, and J. Mellema, Rev. Sci. Instrum. **69**, 1391 (1998).
[7] R. C. Oberthür, Inst. Phys. Conf. Ser. **64**, 321 (1983).
[8] P. Lindner and R. C. Oberthür, Rev. Phys. Appl. **19**, 759 (1984).
[9] B. J. Ackerson, J. B. Hayter, N. A. Clark, and L. Cotter, J. Chem. Phys. **84**, 2344 (1986).
[10] S. J. Johnson, C. G. de Kruif, and R. P. May, J. Chem. Phys. **89**, 5909 (1988).
[11] G. C. Straty, J. Rehabil. Res. Dev. **94**, 259 (1989).
[12] P. G. Cummings, E. Staples, B. Millen, and J. Penfold, J. Meas. Sci. Technol. **1**, 179 (1990).
[13] A. I. Nakatani, H. Kim, and C. C. Han, J. Res. Natl. Inst. Stand. Technol. **95**, 7 (1990).
[14] O. Diat, D. Roux, and F. Nallet, J. Phys. II **3**, 1427 (1993).
[15] K. Mortensen, K. Almdal, F. S. Bates, K. Koppi, M. Tirell, and B. Nordén, Physica B **213&214**, 682 (1995).
[16] V. Schmitt, F. Schosseler, and F. Lequeux, Europhys. Lett. **30**, 31 (1995).
[17] R. J. Plano, C. R. Safinya, E. B. Sirota, and L. J. Wenzel, Rev. Sci. Instrum. **64**, 1309 (1993).
[18] S. J. Johnson, A. J. Salem, and G. G. Fuller, J. Non-Newtonian Fluid Mech. **34**, 89 (1990).
[19] L. Noirez and A. Lapp, Phys. Rev. E **53**, 6115 (1996).
[20] C. Liu and P. J. Puie, Phys. Rev. Lett. **77**, 2121 (1996).
[21] H. Thurn, J. Kalus, and H. Hoffmann, J. Chem. Phys. **80**, 3440 (1984).
[22] B. J. Ackerson and N. A. Clark, Phys. Rev. A **30**, 906 (1984).
[23] L. Herbst, H. Hoffmann, J. Kalus, H. Thurn, K. Ibel, and R. P. May, Chem. Phys. **103**, 437 (1986).
[24] J. Kalus, G. Neubauer, and U. Schmelzer, Rev. Sci. Instrum. **61**, 3384 (1990).
[25] C. G. De Kruif, J. C. van der Werff, S. J. Johnson, and R. P. May, Phys. Fluids A **2**, 1545 (1990).
[26] Y. D. Yan and J. K. G. Dhont, Physica A **198**, 78 (1993).
[27] I. A. Kadoma and J. W. van Egmond, Phys. Rev. Lett. **76**, 4432 (1996).
[28] J. A. Pople and G. R. Mitchell, Liq. Cryst. **23**, 467 (1997).
[29] Ch. Dux, S. Musa, V. Rens, H. Versmold, D. Schwahn, and P. Lindner, J. Chem. Phys. **109**, 2556 (1998).
[30] E. M. Andresen and G. R. Mitchell, Europhys. Lett. **43**, 296 (1998).
[31] S. J. Henderson, J. Appl. Crystallogr. **28**, 820 (1995).
[32] K. Pressl, M. Kriechbaum, M. Steinhart, and P. Laggner, Rev. Sci. Instrum. **68**, 4588 (1997).
[33] A. Guinier and G. Fournet, *Small-Angle Scattering of X Rays* (Wiley, New York, 1955).
[34] G. Fröba and J. Kalus, J. Phys. Chem. **99**, 14450 (1995).
[35] K. Reizlein and H. Hoffmann, Prog. Colloid Polym. Sci. **69**, 83 (1984).
[36] M. Angel, H. Hoffmann, U. Krämer, and H. Thurn, Ber. Bunsenges. Phys. Chem. **93**, 184 (1989).